INDIUM CORPORATION
TECHNICAL PAPER

Achieving Low-Porosity Sintering of Nano-Ag Paste via a Pressureless Process

Authored by: Dr. Ning-Cheng Lee, Sihai Chen, Guangyu Fan, Christine LaBarbera, and Lee Kresge, Indium Corporation, and Xue Yan.

Abstract

A novel nano-Ag sintering paste C has been developed for a pressureless sintering process under air. Paste C was sintered at 250°C (C1) and 280°C (C2), respectively. C1 showed a slightly higher porosity, but a higher shear strength after aging at 250°C for 840 hours. Both C1 and C2 exhibited a microstructure much more stable than the control solder 92.5Pb/5Sn/2.5Ag, which sustained both IMC spalling after thermal aging and voiding. Ag migration toward the DBC to form a dense layer of AgCuNi(Au) was observed for all nano-Ag pastes studied, with C1 and C2 being more moderate in the migration rate. The Ag migration could be attributed to the tendency of Ag to alloy with Au, Ni, and Cu at the DBC side, and may be affected by the chemistry of nano-Ag paste. The porosity of sintered joints was lower toward the center of the die, due to the venting route. The porosity was also lower with a higher bondline thickness, due to a reduced tension in the joint. Thermal aging time has a negligible effect on porosity, presumably due to a balanced stress between tension and sintering shrinkage. The maximum service temperature of the Ag-sintered joint is about 470°C, versus 230°C for high-Pb joints. A liquid-to-liquid thermal shock test from -45 to 240°C was attempted, and was considered too harsh for the die/DBC system employed in this study.

Introduction

Die-attach for high power devices, such as IGBT, is facing increasing challenges of service temperature, thermal conductivity, electrical conductivity, and reliability. Conventional high-lead solder materials are reaching their limitation of performance. Recently, sintering of Ag paste has been advocated as a technology to meet this new challenge. In general, this technology prints the Ag paste on top of a direct bond copper substrate, followed by drying, die placement, and heating under a pressure up to 50MPa. The high pressure is applied in order to avoid formation of high porosity within the Ag joint [1, 2, 3]. The need for high pressure during sintering requires the acquisition of expensive equipment and, inevitably, results in low through-put. Some Ag pastes incorporate polymeric ingredients to avoid the need for pressure, at a cost of high-Ag porosity and a low tolerance for high service temperatures. In this study, a novel Ag-paste without any polymeric inclusion has been developed for the pressureless sintering die-attach process. The sintered joints exhibit high shear strength and a high tolerance toward the high-temperature aging treatment, thus enabling the continuation for advancement of high power devices at a low conversion cost. The morphology and reliability of the sintered joint will be presented and discussed.

DR. NING-CHENG LEE

Dr. Ning-Cheng Lee is a world-renowned soldering expert, an SMTA Member of Distinction, and IEEE Fellow. He has extensive experience in the development of fluxes, alloys, and solder pastes for SMT industries, and extensive experience in the development of high-temperature polymers, encapsulants for microelectronics, underfills, and adhesives.

email: nclee@indium.com
Full biography:
www.indium.com/biographies

Test Regimes

Assembly

Ag Sintering Pastes

Seven nano-Ag sintering pastes were evaluated, including C1, C2, F1, F2, Y1, Y2, Y3, and Y4. C1 and C2 were the same nano-Ag paste C, with C1 referring to the paste sintered at 250°C, and C2 referring to the paste sintered at 280°C. Also included was the 92.5Pb/5Sn/2.5Ag solder paste as the control. For all sintering pastes, a pressureless sintering process was used, with a customized sintering profile for each paste. The high-Pb solder paste used had an 89% metal load and type 3 powder.

Die-Attach Parts

Unless otherwise specified, the die and DBC used were as follows:

- Silicon die size: 3mm x 3mm; surface finish: 750A Ti + 3kA Ni + 750A Ag
- DBC size: 0.925" x 0.925"; ceramic thickness: 0.015"; Cu: 0.008" on both sides with Ni layer thickness of 3.5µm, Au 200nm

Die-Attach Process

In general, the sintering paste was printed onto the DBC, followed by die placement onto the printed paste. The sandwich was then sent through the preferred heating profile under air atmosphere without pressure. For the high-Pb solder paste, the reflow was conducted under nitrogen.

Sample Treatment

Thermal Aging

The attached die was subjected to a 250°C aging treatment for a series of pre-specified times prior to further testing.

Thermal Shock

- Test condition: -45°C/+240°C, liquid-to-liquid
- Time of each cycle: 10min
- Die size: 3mm x 3mm
- DBC size: 0.5" x 0.5"

Sample Testing

Shear Test

After thermal aging or thermal shock treatment, the die was tested for shear strength at an ambient temperature for all materials. For C1 and high-Pb samples, the die was sheared at various temperatures up to 300°C to determine the maximum service temperature.

Morphology Analysis

After the shear test, the parts were examined by optical microscopy and SEM for fracture morphology, and further cross-sectioned for microstructure analysis via SEM and EDS. As a control, some of the samples were cross-sectioned without running through the shear test.

Summary

Shear Strength

The shear strength of various die-attach materials as a result of 250°C aging time are shown in Figure 1. The high-Pb solder paste showed the least strength, although it maintained a relatively stable strength up to about 840 hours. Most of the Ag pastes showed a higher strength than the high-Pb paste

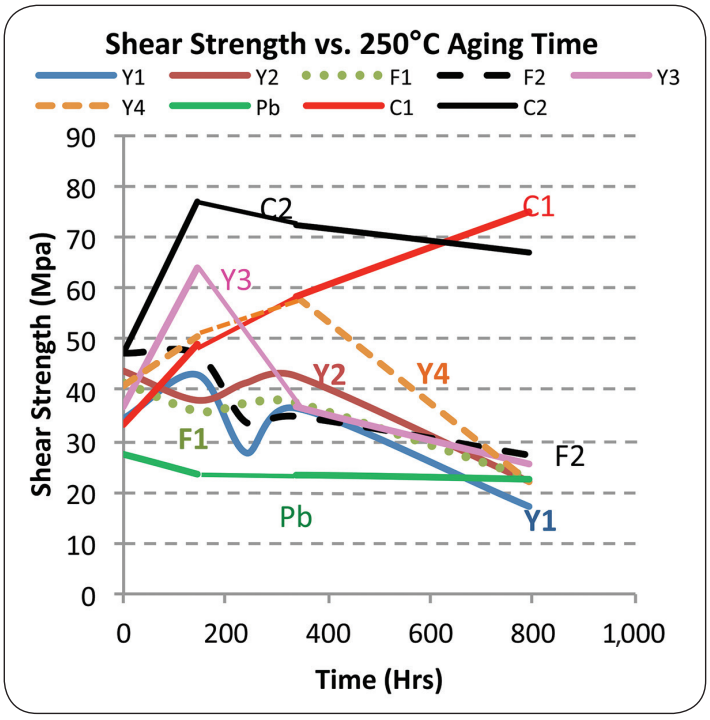

Figure 1. Relationship between shear strength, paste type, and aging time.

at the early phase, but the strength decreased to the level of high-Pb at a later stage. However, the strength of C1 increased continuously with increasing aging time, while C2 reached high strength early and maintained a fairly high strength with aging. Both C1 and C2 displayed strength and stability considerably higher than the rest of the samples, including the high-Pb control. For C1 and high-Pb samples, the shear strength test was conducted up to 3,200 hours aging time at 250°C, as shown in Figure 2. The shear strength of Ag

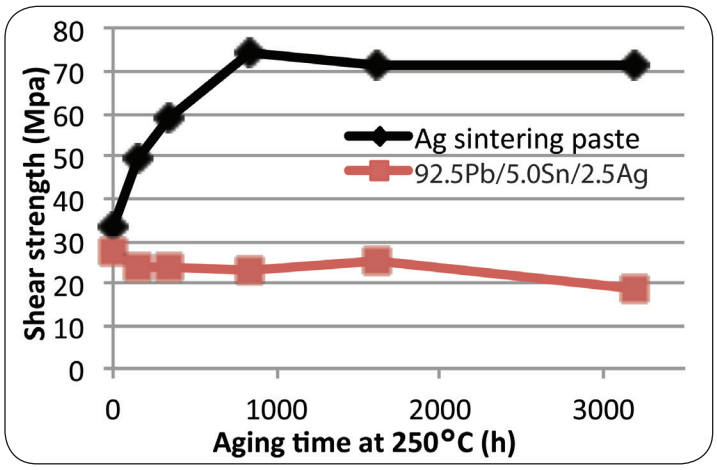

Figure 2. Shear strength of C1 Ag sintering paste and high-Pb sample when aged at 250°C up to 3,200 hours.

sintering paste C1 increased with aging time up to about 800 hours, presumably due to continuous sintering at the aging temperature. Afterward, the shear strength leveled around 70MPa, indicating a very stable joint at 250°C. The shear strength of high-Pb joints showed a moderate decline in strength after 1,600 hours.

Fracture Surface

The fracture surface morphology on the die side for C1, C2, Y3, and high-Pb samples which had been aged at 250°C for 0, 336, and 840 hours is shown in Figure 3. It is interesting to note that for C1 and C2, the "as sintered" texture retained many fine particle shapes. These fine particles sintered further upon aging and achieved a fairly coarse texture after 840 hours aging. This is consistent with increasing strength and increasing aging time, particularly in the case of C1. On the other hand, Y3 achieved a greater extent of sintering in the "as sintered" texture. Further aging only resulted in a slightly more coarse structure. For the high-Pb solder joint, the texture became slightly coarser with aging, suggesting an ongoing grain coarsening process. Furthermore, considerable voiding was observed for the high-Pb solder joints.

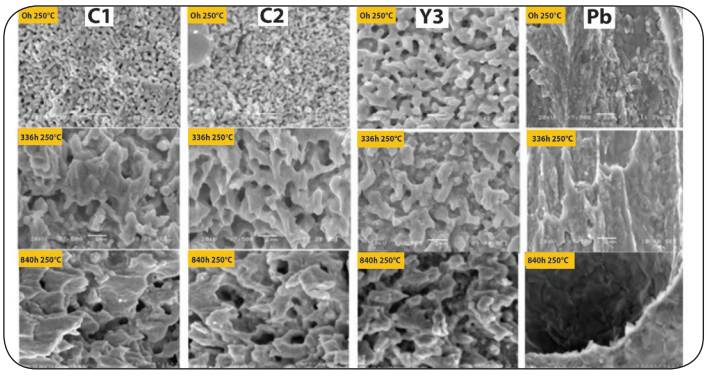

Figure 3. The fracture surface morphology on the die side for C1, C2, Y3, and high-Pb samples, which had been aged at 250°C for 0, 336, and 840 hours.

Ag Migration

For C1 and C2, the sintered joints initially exhibited a fairly uniform porous texture between the die and DBC. With increasing thermal aging time, Ag diffused and deposited onto the DBC and formed a dense layer, while the contact with die was still uniform and the porosity became higher, as shown in Figure 4. For Y3, a dense Ag layer on the DBC surface formed in the "as sintered" state. With increasing aging, Ag deposited on the DBC formed a thick, dense layer. At 840 hours, the contact of the Ag layer with the die became scarce, and only spotty contact remained. This explained the rapid reduction in shear strength for the Y3 system.

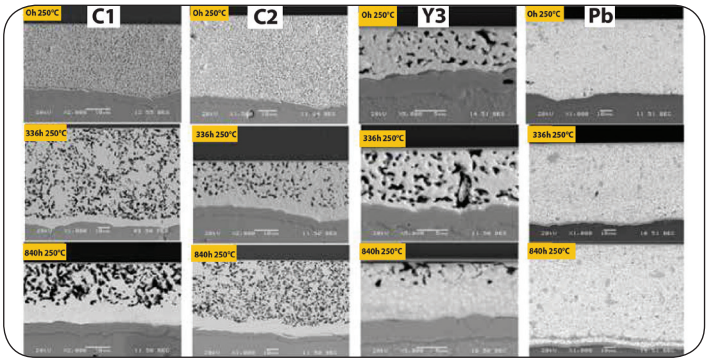

Figure 4. Cross-sectional view of joints of various pastes after aging treatment.

The Ag migration from the bulk joint toward the DBC side can be viewed more clearly in Figure 5. After the shear test was conducted, the die on the DBC parts were cross-sectioned and placed face-to-face between the die and the DBC. For C1 and C2, the "as sintered" joints fractured near the DBC surface. With increased thermal aging, more and more Ag diffused toward the DBC and formed a dense layer on top of the DBC. However, even after 840 hours of aging, significant Ag still bonded strongly to the die surface and the shear fracture occurred within the bulk Ag joint. The same could not be said for the Y3 sample; very little Ag could be found on die surface after thermal aging for 840 hours. This explained the significant reduction of shear strength after 840 hours of thermal aging.

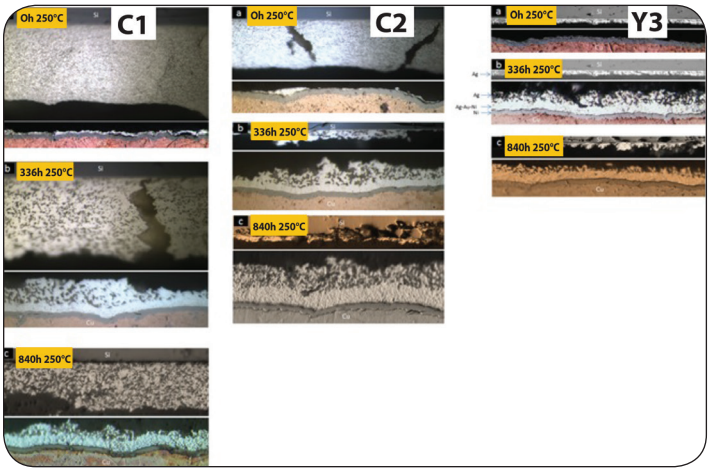

Figure 5. The die on the DBC parts after the shear test were cross-sectioned and placed face-to-face between the die and the DBC.

The diffusion of Ag toward the DBC to form a dense layer was further investigated by examining the composition of the Ag joint. Figure 6 shows the C1 and Y4 joints. For sample C1, in the dense layer on top of DBC point 4, the atomic composition is 97.84Ag/1.33Cu/0.84Ni. For both point 2 and point 3, the composition is 100Ag. For the Y4 joint, in the dense layer on top of the DBC, the atomic composition is 91.01Ag/2.18Cu/4.80Ni/2.01Au for point 4. For both points 2 and 3, the composition is AgCuNi. Presumably, the tendency for Ag to migrate to the DBC to form a dense layer is driven by the tendency for Ag to alloy with Ni, Cu, and Au. The supply of Ni on the die side is very limited due to the thin layer of Ni on the die, but the Ni and Cu supply is plenty on the DBC side. As a result, Ag in the joint continuously migrated to the DBC side to form a dense alloy layer.

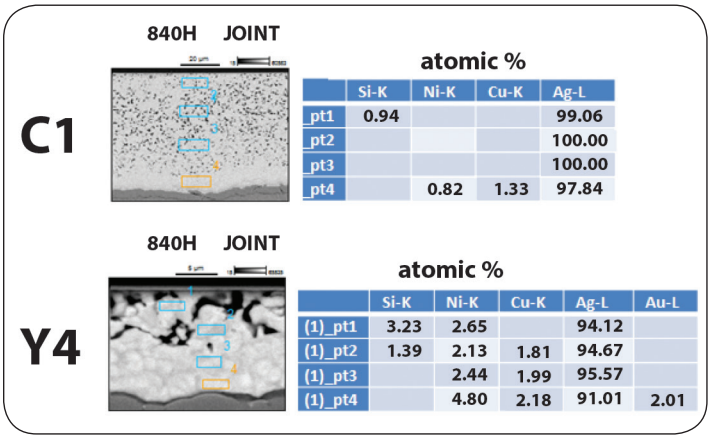

	Si-K	Ni-K	Cu-K	Ag-L
pt1	0.94			99.06
pt2				100.00
pt3				100.00
pt4		0.82	1.33	97.84

	Si-K	Ni-K	Cu-K	Ag-L	Au-L
(1)_pt1	3.23	2.65		94.12	
(1)_pt2	1.39	2.13	1.81	94.67	
(1)_pt3		2.44	1.99	95.57	
(1)_pt4		4.80	2.18	91.01	2.01

Figure 6. Composition of C1 and Y4 Ag joints aged at 250°C for 840 hours.

Porosity

Bondline Porosity Distribution

Upon sintering, it was noticed that the porosity distribution along the bondline was uneven, as shown in Figure 7. Here, the die was attached with C1 Ag-sintering paste and was aged at 250°C for 3,200 hours. The porosity of the joint appeared to be higher at both ends and lower toward the center.

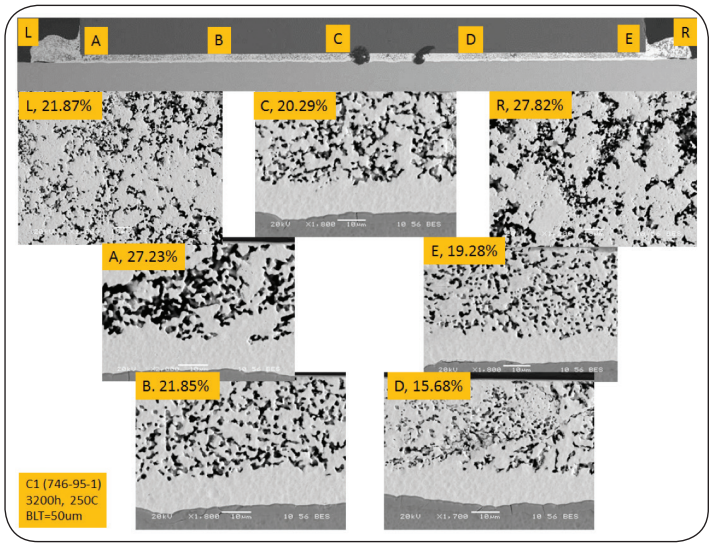

Figure 7. Porosity distribution along 3mm x 3mm die bondline for joint using C1 Ag sintering paste aged at 250°C for 3,200 hours.

Table 1 shows the porosity of sintered joints along the bondline for dies attached with C1 Ag-sintering paste and aged at 250°C for various times. The average of porosity and bondline thicknesses for the bondline under the die is calculated and is also shown in Table 1.

Figure 8 shows the relationship between porosity and location of joint under the die for dies attached with C1 Ag-sintering paste. The samples have been aged at 250°C for various amounts of time.

In most instances, the porosity toward the center was lower than the edge. This may be caused by the outgassing factor at sintering. Presence of vapor is expected to hamper the sintering. Upon sintering, the organic materials vaporized, and the only venting route was toward the edge. With the vapor moving toward the edge, the vapor will diminish from the center first, thus resulting in a lower porosity at the center.

Table 1. Porosity of sintered joints along bondline for dies attached with C1 Ag-sintering paste and aged at 250°C for various times. Also shown are the average of porosity and bondline thickness.

Location	250°C Aging Time					
	0hr	144hr	336hr	840hr	1,608hr	3,200hr
L (Outer Left)	30.54	--	28.14	21.47	--	21.87
A (Edge)	28.24	25.14	19.24	24.86	17.61	27.23
B	26.2	2.54	18.58	28.69	9.86	21.85
C (Center)	24.83	2.28	22.98	26.53	10.19	20.29
D	26.64	1.46	22.61	24.5	9.76	15.68
E (Edge)	30.84	23.21	29.76	24.91	25.12	19.28
R (Outer Right)	30.92	--	30.03	21.04	28.62	27.82
Porosity Average Under Die (A to E, %)	27.4	10.9	22.6	25.9	14.5	20.9
Bondline Thickness (μ)	32	82	76	25	70	50

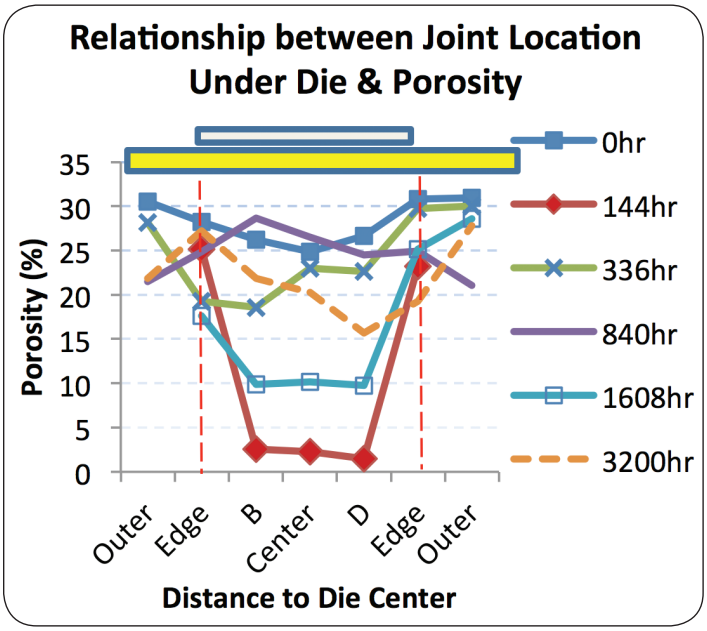

Figure 8. Relationship between porosity and location of joint under the die for dies attached with C1 Ag-sintering paste.

Bondline Thickness Effect

The bondline thickness of nano-Ag paste appeared to have an affect on the migration behavior. As shown in Figures 4 and 5, the bondline thickness of Y3 was around 10μm. With Ag migrated toward the DBC, porosity concentrated near the die side and resulted in joint rupture near the die surface, as shown in Figure 5. The bondline thickness of C1 and C2 mostly ranged from 40–50 microns, as shown in Figure 4. With plenty Ag supply available for migration, the porosity concentration phenomenon became much more moderate and the joint ruptured within the bulk body of the sintered joint, instead of near the die surface.

It should be noted that although samples in Table 1 all utilized C1 Ag-sintering paste, the bondline thickness did vary from one specimen to another due to variation in the die placement process. The effect of bondline thickness on porosity was further investigated by examining the porosity of C1 sintered joints, regardless of the 250°C aging history.

Although some data scattering is observed, the porosity clearly increases with decreasing bondline thickness with an R-squared value 0.66. The high porosity associated with a thinner bondline could be attributed to the tension of bonding. Upon sintering, the Ag-paste volume gradually decreased with increasing extent of sintering. However, the dimensions of both the die and DBC did not change. With Ag paste bonded to the surface of both the die and DBC, the shrinking volume of Ag paste at sintering and the fixed dimension of the die and DBC inevitably resulted in a tension within the joint. The thinner the bondline, the higher the tension would be. The tension exerted onto the Ag joint suppressed the shrinking tendency of sintering, and consequently resulted in a higher porosity.

Thermal Aging Time Effect

The samples in Figure 9 involved various aging times at 250°C. In order to clarify the trend caused by bondline thickness or aging time, the porosity of C1 samples in Table 1 was also plotted against the 250°C aging time, with results shown in Figure 10. Apparently, the high temperature aging time virtually had no affect on porosity, as reflected by the low R-square value of 0.0091.

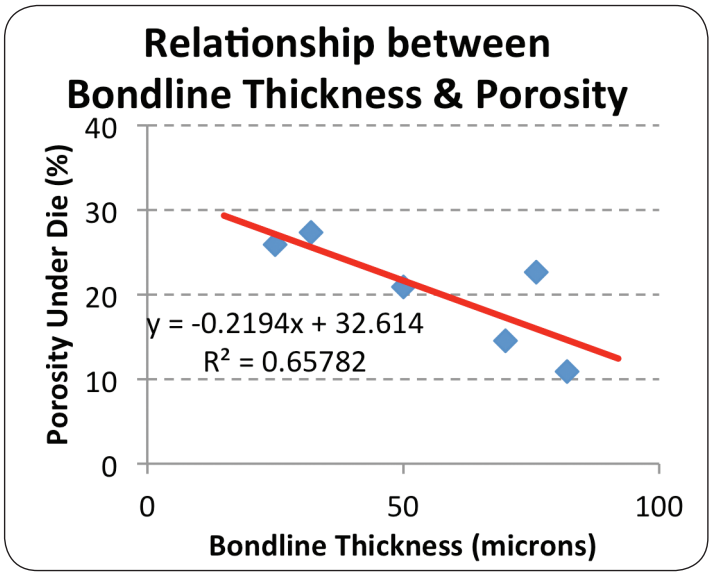

Figure 9. Relationship between porosity and bondline thickness for dies attached with C1 Ag-sintered paste aged at 250°C for various amounts of time.

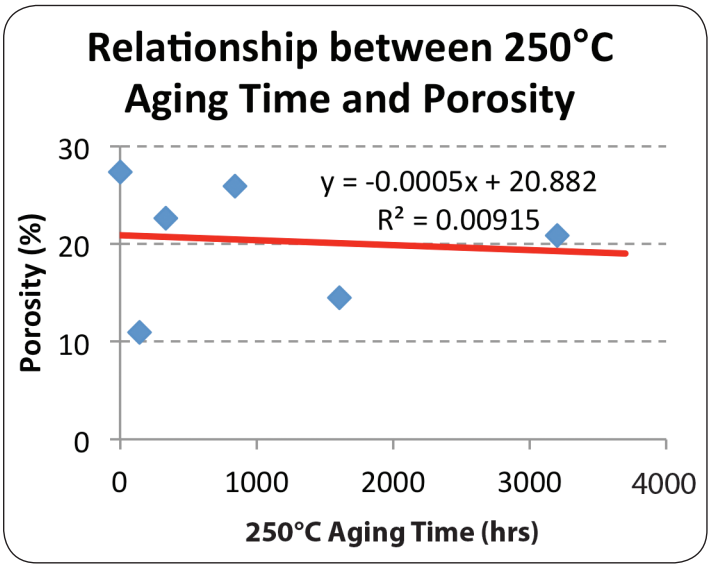

Figure 10. Effect of 250°C aging time on porosity of C1 Ag-sintered joints.

The insignificant effect of thermal aging time on porosity indicated that the sintering shrinkage became negligible after the sintering die bonding process, presumably due to the balanced stress between tension and shrinkage. The findings here confirmed that the trend observed in Figure 9 was mainly attributed to the bondline thickness effect.

The insignificant effect of thermal aging time on porosity also indicates that increasing the shear strength of the C1 joint with increasing aging time in Figure 2 was not caused by a reduction in porosity. Instead, it could be attributed to a better microscopic continuity of the Ag phase, as shown in Figure 4. Although the porosity did not decrease, the porosity distribution did evolve from microscopic homogeneity to macroscopic homogeneity, in addition to the emergence of a dense Ag alloy zone on top of the DBC surface.

High-Pb Joint

In Figure 4, the high-Pb solder joint appears to be very uniform. However, at 840 hours, a belt structure near the DBC surface was observed.

A close-up look of the high-Pb solder joint after aging at 250°C for 840 hours is shown in Figure 11, together with EDS analysis on several areas in the picture. Area 1 indicates that this is mainly the NiCuSn IMC; area 2 has a fairly high Pb content; area 3 is the Ni3/Sn4 IMC layer; and area 4 is the electroless Ni(P) layer. The formation of individual phases can be attributed to the following mechanism. First, Sn in 92.5Pb/5Sn/2.5Ag reacted with Ni, forming the Ni_3Sn_4 IMC layer. The interaction with Cu, which came from the diffusion through the Ni layer, resulted in NiCuSn IMC. Upon aging, this NiCuSn IMC layer spalled off from the Ni3/Sn4 surface and formed a separate IMC belt. This spalling phenomenon signaled deterioration of joint stability, which could eventually result in voids or cracks near the solder joint interface. In other words, the high-Pb solder joints showed signs of deterioration of reliability after aging at 250°C for 840 hours.

After 3,200 hours of aging at 250°C, a shear strength decrease of 32% for the 92.5Pb/5.0Sn/2.5Ag joint was observed in Figure 2. A cross-section of the joint shows voids along the Si side. Cracks are observed between the voids, as shown in Figure 12. EDS analysis indicated Ni_3Sn_4 IMC formed at the interface between the solder and Ni layer. The irregularly-shaped voids that were formed could be attributed to the depletion of Sn and shrinkage caused by recrystallization of high-Pb solder. Cracks are present near the interface of the solder and the die, presumably initiated from the voids, and then propagated between the voids.

The voiding and crack of the 92.5Pb/5.0Sn/2.5Ag joint indicates that the joint appeared to be near a catastrophic failure after 3,200 hours aging at 250°C, although the shear strength decrease was relatively moderate.

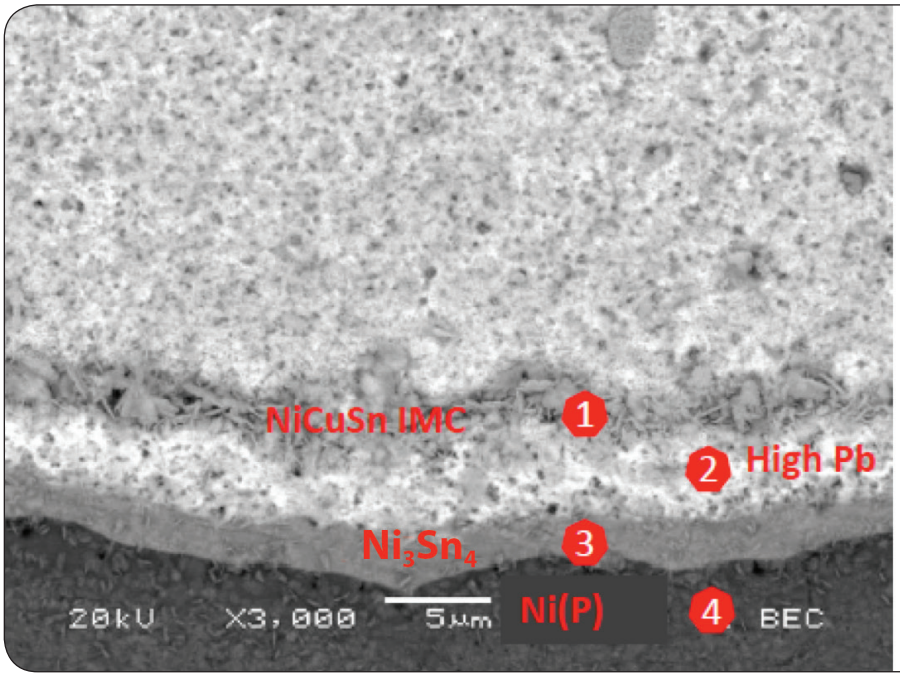

Element Of Point 1	Atom %
C K	65.35
O K	16.13
Al K	1.84
Ni K	0.26
Cu K	0.37
Sn L	0.54
Pb L	15.53
Total	100.00

Element Of Point 2	Atom %
O K	37.42
Al K	5.75
Ni K	1.08
Cu K	1.55
Pd L	2.03
Sn L	2.08
Pb L	50.09
Total	100.00

Element Of Point 3	Atom %
C K	42.29
O K	4.49
Ni K	21.28
Cu K	1.15
Sn L	29.17
Pb L	1.62
Total	100.00

Element Of Point 4	Atom %
C K	52.41
O K	3.13
P K	6.22
Ni K	36.37
Cu K	0.76
Pb L	1.11
Total	100.00

Figure 11. Effect of 250°C aging time on porosity of C1 Ag-sintered joints.

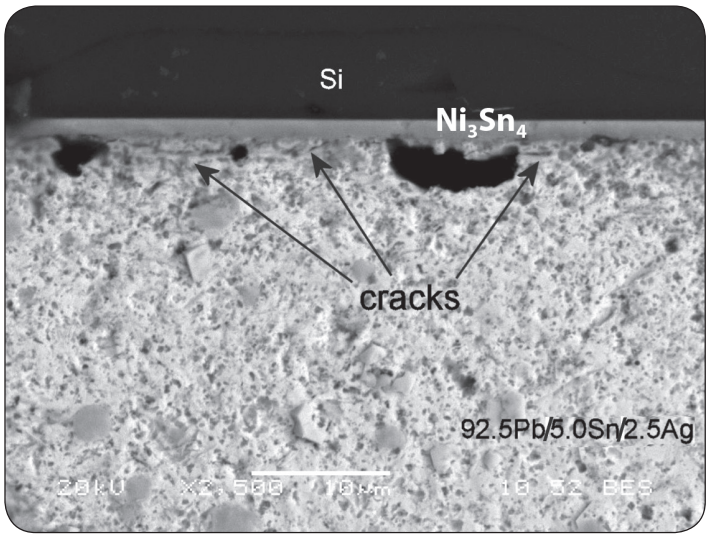

Figure 12. A close-up look of the high-Pb solder joint after aging at 250°C for 3,200 hours.

Thermal Shock

The F1 sample was subjected to thermal shock treatment and then followed by the shear test and fracture surface analysis. Figure 13 shows the sheared F1 sample without thermal shock treatment. Figure 14 shows the sheared F1 sample after 100 cycles of thermal shock pretreatment.

Delamination of the silver layer from the metallization layers on the die backside near the edge was observed, which was confirmed by EDS, as shown in Figure 14. Au and Ni were detected by EDS in the middle of the sintered silver area on the

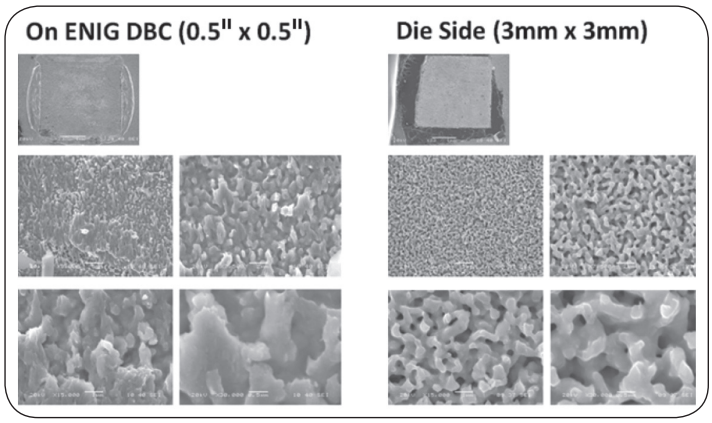

Figure 13. The sheared F1 sample without thermal shock treatment.

ENIG DBC and the die backside. This implies that the sintered joints partially peeled off from the substrate. After 100 cycles of -45°C/+240°C, many crack lines showed up on the sintered silver layer, and the morphology of joints dramatically changed, as shown in Figure 14. In conclusion, the delamination of a silver layer from the backside of the die is the root cause of failure in thermal shock tests.

Parallel to this test, a blank DBC coupon 0.925" x 0.925" was also subject to thermal shock. It was found that the Cu layer delaminated from the ceramic core in less than 100 cycles. This result suggested that this thermal shock test condition was too harsh for a reliability study of the die on the DBC.

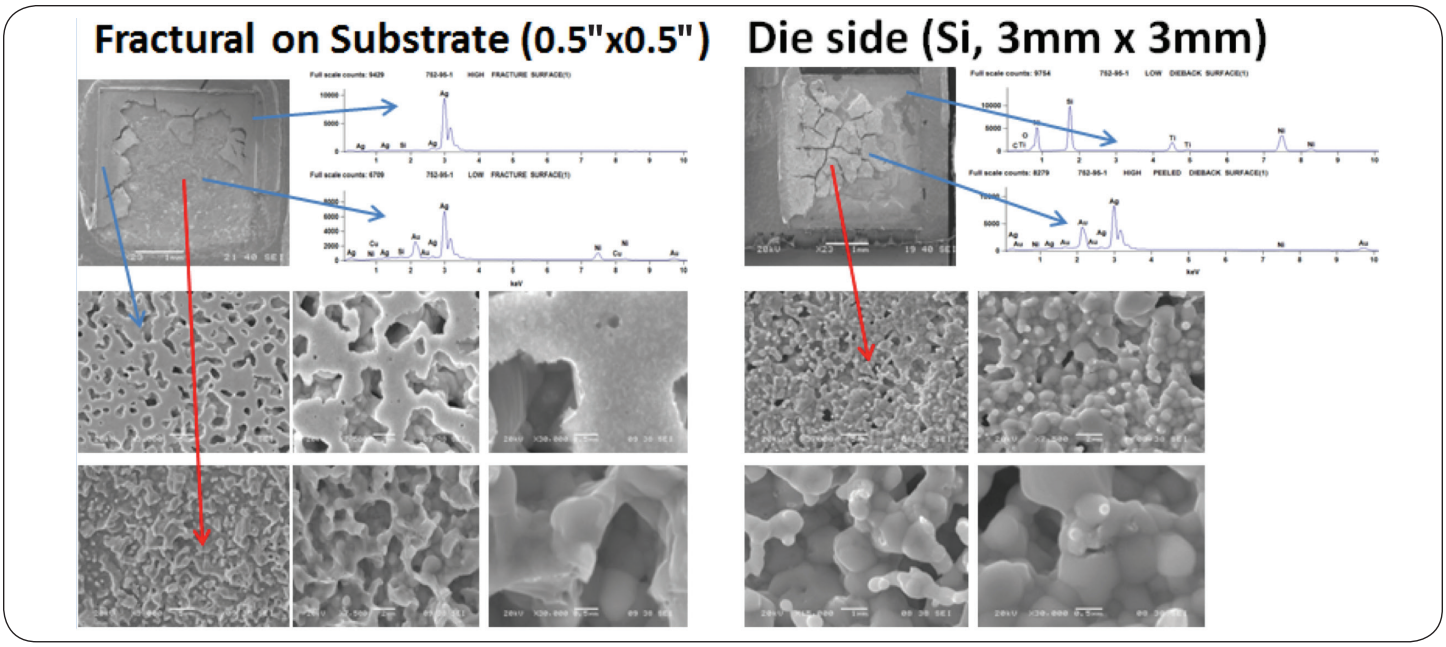

Figure 14. The sheared F1 sample after 100 cycles of thermal shock pretreatment.

Service Temperature

The service temperature of C1 Ag-sintered paste and high-Pb solder was determined by running a shear test up to 300°C, with results shown in Figure 15. By using 6.1MPa die shear strength as the pass criteria for high-Pb solder joints, of which the melting temperature range is 287–296°C, the maximum service temperature is about 230°C. On the other hand, the Ag-sintered joints exhibited a very high shear strength of at least up to 300°C, and the extrapolated shear strength indicated a maximum service temperature of 470°C.

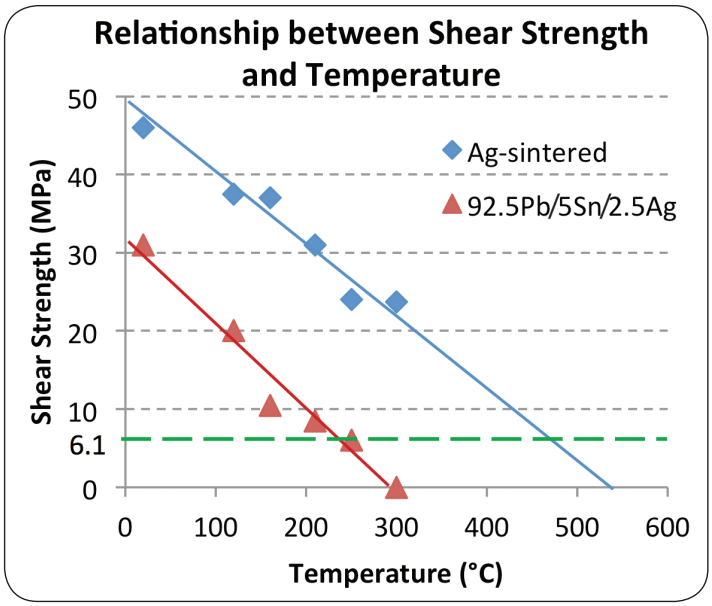

Figure 15. Shear strength of C1 Ag-sintered joint and 92.5Pb/5Sn/2.5Ag joints at various testing temperature.

Discussion

Effects of Sintering Temperatures

C1 showed the shear strength increased with increasing aging time, while C2 reached a maximum after 6 days, then decreased slightly with increasing aging. In the case of C1 and C2, the nano-Ag sintering paste employed were the same. The difference in the shear strength behavior can be attributed to a higher internal stress of C2 caused by a higher sintering temperature of 280°C. Although the porosity of C1 is slightly higher than C2, the benefit of a lower internal stress appears to outweigh the higher porosity disadvantage.

Sintering Profile

In this study, a customized pressureless sintering profile was used for each Ag-sintering paste. However, it has been recognized that the desired sintering profile may vary with die size, as well. For instance, for C1 sintering paste, the desired sintering profile for 3mm x 3mm die and 10mm x 10mm die are shown in Figure 16. For large die, the preferred profile is longer than that for a small die.

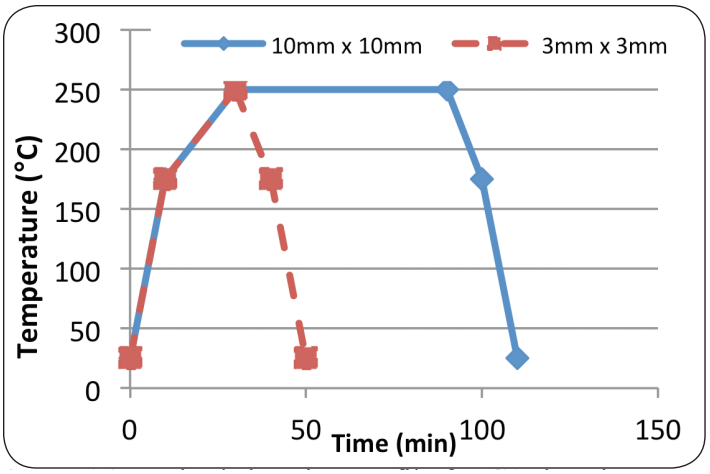

Figure 16. Desired sintering profile for C1 sintering paste.

Conclusion

A novel nano-Ag sintering paste C has been developed for a pressureless sintering process under air. Paste C was sintered at 250°C (C1) and 280°C (C2), respectively. C1 showed a slightly higher porosity, but a higher shear strength after aging at 250°C for 840 hours. Both C1 and C2 exhibited a microstructure much more stable than the control solder 92.5Pb/5Sn/2.5Ag, which suffered both IMC spalling after thermal aging and voiding. Ag migration toward the DBC to form a dense layer of AgCuNi(Au) was observed for all nano-Ag pastes studied, with C1 and C2 being more moderate in the migration rate. The Ag migration could be attributed to the tendency of Ag to alloy with Au, Ni, and Cu at the DBC side, and may be affected by the chemistry of nano-Ag paste. The porosity of sintered joints was lower toward the center of die, due to the venting route. The porosity was also lower with a higher bondline thickness, due to a reduced tension in the joint. Thermal aging time has a negligible effect on porosity, presumably due to the balanced stress between tension and sintering shrinkage. The maximum service temperature of a Ag sintered joint is about 470°C, versus 230°C for high-Pb joints. A liquid-to-liquid thermal shock test from -45 to 240°C was attempted, and was considered too harsh for the die/DBC system employed in this study.

References

1. Kim S. Siow (Onsemi), "Mechanical properties of nano-silver joints as die-attach materials," Journal of Alloys and Compounds 514 (2012) 6–19.
2. Jianfeng Yan, Guisheng Zou, Ai-ping Wu, Jialie Ren, Jiuchun Yan, Anming Huc and Y. Zhoua, "Pressureless bonding process using Ag nanoparticle paste for flexible electronics packaging." Available online at www.sciencedirect.com; Scripta Materialia 66 (2012) 582–585.
3. Soichi Sakamoto and Katuaki Suganuma (Osaka Univ), "Thermo Mechanical Reliability of Low-temperature Low-pressure Die Bonding Using Thin Ag Flake Pastes," CIPS 2012, March 6–8, 2012, Nuremberg, Germany.

First presented at ECTC 2015.